

# NNLO QCD predictions for $W\gamma\gamma$ production at the LHC

Paolo Garbarino<sup>(a)</sup>, Massimiliano Grazzini<sup>(a)</sup>,  
Stefan Kallweit<sup>(a)</sup> and Chiara Savoini<sup>(b)</sup>

<sup>(a)</sup> Physik Institut, Universität Zürich, Winterthurerstrasse 190, 8057 Zürich, Switzerland

<sup>(b)</sup> Physics Department, TUM School of Natural Sciences, Technical University of Munich,  
James-Frank-Straße 1, 85748 Garching, Germany

## Abstract

Triboson production processes play a crucial role in probing the electroweak sector of the Standard Model, as they involve quartic gauge-boson couplings already at the tree level. With these measurements entering the precision era at the Large Hadron Collider (LHC), accurate theoretical predictions become indispensable. We present the computation of the next-to-next-to-leading-order (NNLO) QCD radiative corrections to the production of a  $W$  boson in association with two photons ( $W\gamma\gamma$ ) at the LHC. The calculation is exact, except for the finite part of the two-loop contribution, which is included in the leading-colour approximation. Predictions for the fiducial cross section and selected kinematic distributions are provided at a centre-of-mass energy of  $\sqrt{s} = 13$  TeV, under standard experimental selection cuts. In line with observations for other multiboson processes involving direct photons, we find sizable NNLO corrections that enhance the next-to-leading-order predictions by about 23%, with residual perturbative uncertainties that can be roughly estimated to be at the 5% level.

# 1 Introduction

Over the past decade, precision measurements at the LHC have enabled detailed studies of the trilinear couplings of electroweak (EW) gauge bosons through diboson production. To achieve a precise understanding of the EW symmetry breaking within the Standard Model (SM), the quartic couplings must likewise be scrutinised with a comparable level of accuracy. This requires a more refined investigation of triboson production processes, which — together with diboson production via weak-boson scattering — already probe quartic gauge couplings at the tree level. Deviations from SM predictions could thus directly point to effects of new physics in the EW sector. Moreover, triboson processes constitute a dominant background to other key SM processes. For example,  $V\gamma\gamma$  ( $V = Z, W$ ) production is an irreducible background to  $VH$  production via Higgsstrahlung, with the Higgs boson decaying into two photons. Despite their significantly smaller cross sections, triboson processes are now within reach at the LHC, making reliable theoretical predictions essential. Among the first processes of the triboson class,  $V\gamma\gamma$  production has been measured both at 8 TeV and 13 TeV by ATLAS and CMS, as reported in Refs. [1, 2] and [3, 4], respectively.

On the theory side, next-to-leading-order (NLO) QCD corrections to triboson production have been computed mainly for leptonic decay channels [5–14], and have proven essential for reducing the gap between predictions and experimental measurements. Triboson production in SM Effective Field Theory (SMEFT) at NLO QCD was studied in Ref. [15]. Complete NLO EW corrections, mostly including fully leptonic decays of the heavy gauge bosons, are available for some relevant triboson processes [16–20]. Those involving two or more final-state photons, i.e. triphoton and  $V\gamma\gamma$  production, have been discussed in Ref. [21]. NNLO QCD corrections are expected to be important, owing to the close similarity with diboson production processes, where they have been shown to yield sizeable and positive effects, especially in the presence of final-state photons [22–29]. Indeed, in the case of triphoton production — the only triboson process for which NNLO QCD predictions are currently available [30, 31]\* — very large NNLO corrections of  $\mathcal{O}(60\%)$  relative to the NLO prediction have been observed at the level of fiducial cross sections. It was also shown that good agreement with the data measured by the ATLAS collaboration [33] could only be achieved by including those corrections.

While tree-level and one-loop amplitudes can be obtained using automated tools, a complete NNLO QCD computation is typically limited by the availability of the corresponding two-loop amplitudes, whose complexity grows rapidly with the number of (massive or off-shell) legs. Until recently, in the class of triboson processes, only the two-loop amplitudes for triphoton production, involving exclusively massless external legs, were available first in the leading-colour approximation (LCA) [30, 31] and later supplemented by all subleading-colour structures [32]. In Ref. [34], the first computation of the two-loop amplitudes for a triboson process with one off-shell leg, namely  $W\gamma\gamma$  production, has been reported. In this Letter, we present the first NNLO QCD predictions for  $W\gamma\gamma$ , exploiting these two-loop amplitudes and the implementation of the  $q_T$ -

---

\* These predictions rely on a leading-colour approximation of the relevant two-loop amplitudes. Complete amplitudes including subleading-colour contributions have been made available in the meanwhile [32].

subtraction formalism [35] in the MATRIX framework [26].<sup>†</sup>

## 2 Computational details

In this Section, we briefly discuss the procedure adopted for the NNLO QCD computation. For brevity, we refer to the process as  $W\gamma\gamma$  production; however, the calculation is performed for the complete leptonic final states, without invoking any resonance approximation. To be precise, in this work we consider both the  $pp \rightarrow \ell^+ \nu_\ell \gamma\gamma$  and  $pp \rightarrow \ell^- \bar{\nu}_\ell \gamma\gamma$  processes. Belonging to the class of colourless final-state systems, the treatment of infrared (IR) singularities can be addressed by applying the standard  $q_T$ -subtraction formalism [35], as implemented in the MATRIX framework [26], which we have suitably extended to deal with massive triboson production. All NLO-type singularities are treated using the dipole-subtraction method [36, 37]. The NNLO computation in the  $q_T$ -subtraction formalism requires the introduction of a technical cut-off,  $r_{\text{cut}}$ , on the dimensionless variable  $r = q_T/Q$ , where  $q_T$  is the transverse momentum of the colourless system and  $Q$  its invariant mass. The prediction for the NNLO fiducial cross section is then obtained by numerically performing the extrapolation  $r_{\text{cut}} \rightarrow 0$ . For distributions, this procedure is applied on a bin-wise level, thereby providing differential results that are free from power corrections in  $r_{\text{cut}}$ . As for the fiducial results, an extrapolation error is assigned. Combined with the statistical error from the phase-space integration, this provides the overall numerical uncertainty. It is well known that the photon-isolation procedure induces a significant  $r_{\text{cut}}$  dependence in the fiducial cross section, with the resulting power corrections being larger for tighter isolation [26, 38]. Nevertheless, as shown e.g. in Ref. [31] for triphoton production, those power corrections are under control at the level of a few permille through the extrapolation approach adopted in MATRIX. In Figure 1, we explicitly display the NLO and NNLO cross sections for  $W^-\gamma\gamma$  production as a function of  $r_{\text{cut}}$ . The extrapolated result for  $r_{\text{cut}} \rightarrow 0$  is also presented, together with the corresponding extrapolation uncertainty (orange band), estimated via the standard MATRIX procedure. For reference, at NLO we include the  $r_{\text{cut}}$ -independent result (red line) obtained with dipole subtraction. We find perfect agreement between the two subtraction methods at the sub-permille level at NLO. The numerical stability of our results allows us to conservatively assign a numerical error of a few permille to the predicted fiducial NNLO cross section.

The computation within the MATRIX framework is fully automated. Also the evaluation of tree-level and one-loop amplitudes relies on automated tools like OPENLOOPS [39–41] and RECOLA [42–44]. The only ingredient that needs to be treated on a process-by-process basis is represented by the two-loop amplitudes. For  $W\gamma\gamma$ , these amplitudes were recently made available in the LCA [34]. We have implemented the provided results into a dedicated C++ library suitable for numerical evaluation, building on and improving upon the amplitude libraries developed for the calculations in Refs. [45–47].<sup>‡</sup> To ensure the reliability and stability of the amplitudes

---

<sup>†</sup> In this first NNLO computation of  $W\gamma\gamma$  production, we restrict ourselves to the LCA for the two-loop amplitudes. The evaluation of the subleading-colour contributions, available upon request in Ref. [34], is extremely slow, and its inclusion is left for future work.

<sup>‡</sup> The IR-finite remainder of the two-loop amplitude is computed according to the conventions of Ref. [48].

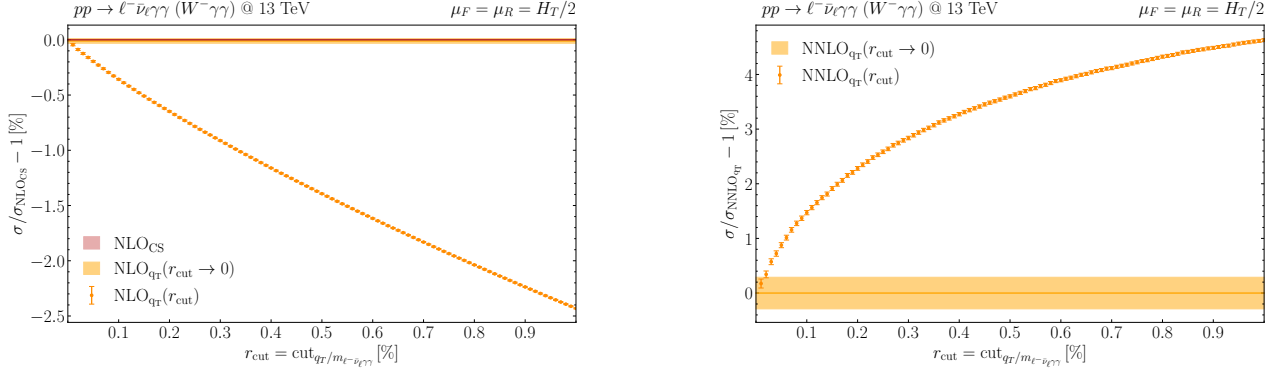


**Figure 1:**  $r_{\text{cut}}$  dependence of the NLO and NNLO cross sections for  $pp \rightarrow \ell^- \bar{\nu}_\ell \gamma \gamma$  (dotted points with errorbars) and the extrapolated result,  $r_{\text{cut}} \rightarrow 0$  (solid), at the central scale  $\mu_F = \mu_R$ .

despite the large numerical cancellations expected at intermediate stages of the calculation, we have introduced a sophisticated numerical rescue system while keeping sustainable runtimes per evaluated phase-space point. By default, we rely on quadruple-precision arithmetic throughout for the evaluation of the rational coefficients of the master integrals, whereas the time-consuming evaluation of the five-point one-mass master integrals is performed in double precision via the `PentagonFunctions++` library [49–52]. The rescue system exploits the symmetry of the amplitude under the exchange of the two photons. Thus, by evaluating the amplitude for both permutations — at the cost of doubling the runtime — we obtain a robust estimate of potential precision loss. Beyond a certain user-defined threshold, the amplitude is re-evaluated at octuple precision for the rational coefficients. Again, this re-evaluation can be performed for both photon permutations, and if a reasonable agreement is still not reached, the precision for the master-integral evaluation is increased to quadruple. This procedure yields numerically stable amplitudes for all considered phase-space points, with an average runtime of approximately six seconds, which is fully acceptable and does not significantly impact the overall computational cost.

### 3 Numerical results

In this Section, we present our predictions for the  $pp \rightarrow \ell \nu_\ell \gamma \gamma$  processes at NNLO in QCD. We consider proton–proton collisions at a centre-of-mass energy of  $\sqrt{s} = 13$  TeV and employ typical fiducial cuts inspired by the recent ATLAS measurement of  $W \gamma \gamma$  production [2]. We use a smooth-cone isolation [53], but slightly adapt the standard threshold ( $E_{T,\text{max}} = \epsilon p_{T,\gamma}$ ) to also account for a constant term ( $E_{T,\text{thres}}$ ), i.e. we define  $E_{T,\text{max}} = \epsilon p_{T,\gamma} + E_{T,\text{thres}}$ . More precisely, for every  $r \leq R$ , where  $r = \sqrt{(\Delta\eta)^2 + (\Delta\phi)^2}$  describes a cone of radius  $r$  around the photon ( $\eta$  and  $\phi$  denote pseudorapidity and azimuth, respectively), we require  $E_{T,\text{had}}(r) \leq E_{T,\text{max}} \left(\frac{1-\cos r}{1-\cos R}\right)^n$ , with  $n = 1$  and  $R = 0.4$ , for the total amount of partonic transverse energy inside the cone. To resemble the fixed-cone criterion used in Ref. [2], we set  $\epsilon = 0.032$  and  $E_{T,\text{thres}} = 6.53$  GeV.

The isolated photons must fulfill  $p_{T,\gamma} > 20$  GeV and  $|\eta_\gamma| < 2.37$ . The charged lepton is required to have  $p_{T,\ell} > 25$  GeV and  $|\eta_\ell| < 2.47$ , while the missing transverse momentum of the event needs

to fulfil  $p_{T,\text{miss}} > 25$  GeV. The conditions  $\Delta R_{\gamma,\ell} > 0.4$  and  $\Delta R_{\gamma,\gamma} > 0.4$  are imposed on the separation between the charged lepton and the photons and between the two photons, respectively. We further impose the condition  $m_T^W > 40$  GeV on the transverse mass of the  $W$  boson, defined as  $m_T^W = \sqrt{2p_{T,\ell}p_{T,\text{miss}}(1 - \cos \Delta\phi)}$  where  $\Delta\phi$  is the difference in azimuthal angles between the lepton momentum and the missing transverse momentum  $p_{T,\text{miss}}$ .

We employ the  $G_\mu$  scheme, and set the input parameters to the PDG values [54]:  $G_F = 1.16639 \times 10^{-5} \text{ GeV}^{-2}$ ,  $m_W = 80.385 \text{ GeV}$ ,  $\Gamma_W = 2.0854 \text{ GeV}$ ,  $m_Z = 91.1876 \text{ GeV}$ , and  $\Gamma_Z = 2.4952 \text{ GeV}$ . We apply the complex-mass scheme [55], and thus compute the EW mixing angle as  $\cos\theta_W^2 = \mu_W^2/\mu_Z^2$ , with  $\mu_V^2 = m_V^2 - i\Gamma_V m_V$  ( $V = W, Z$ ), as well as  $\alpha = \sqrt{2} G_F |\mu_W^2 (1 - \mu_W^2/\mu_Z^2)|/\pi$ . Following the reasoning of Ref. [41], we replace one factor of  $\alpha$  by  $\alpha_0 = 1/137.036$  for each identified final-state photon. We use a diagonal Cabibbo–Kobayashi–Maskawa (CKM) matrix. We work in the 5-flavour scheme and employ the NNPDF40 [56] parton distribution functions (PDFs), with densities and QCD coupling  $\alpha_S$  ( $\alpha_S(m_Z) = 0.118$ ) evaluated at each corresponding order through the LHAPDF interface [57]. We choose the central renormalisation and factorisation scales as  $\mu_R = \mu_F = H_T/2 = (E_{T,\ell\nu} + p_{T,\gamma_1} + p_{T,\gamma_2})/2$ , where  $E_{T,\ell\nu} = \sqrt{m_{\ell\nu}^2 + p_{T,\ell\nu}^2}$ . The scale uncertainties are obtained through the customary procedure of independently varying the renormalisation and factorisation scales by a factor of two around their common central value, with the constraint  $0.5 \leq \mu_R/\mu_F \leq 2$ .

Before presenting our numerical results, we recall some features of QCD radiative corrections for multiboson processes involving direct photons. Exceptionally large NLO and NNLO corrections are observed for diphoton [22, 25, 27], triphoton [30, 31] and  $W\gamma$  [24, 29] production. All these processes are driven by quark–antiquark annihilation at the Born level. The (anti)quark–gluon channel opening up at NLO leads to a significant correction, since its large luminosity can compensate the  $\mathcal{O}(\alpha_S)$  factor. A related and complementary observation is that the LO cross section is often suppressed in specific phase-space regions either for *kinematical* or *dynamical* reasons. In diphoton production with asymmetric cuts on the photon transverse momenta, for example, part of the NLO enhancement can be traced back to the opening of the phase-space region in which the softer photon is radiated close to its kinematic cut [22, 25, 27]. For triphoton production, the regions where the azimuthal separation of the leading and the subleading/trailing photons is small open up only at NLO, due to the selection cuts on the photon transverse momenta [31]. In the case of  $W\gamma$  production, the LO suppression has instead a *dynamical* origin: the LO matrix element vanishes [58] for a certain scattering angle of the  $W$  boson in the partonic centre-of-mass frame. Such *radiation zero* is present also for  $W\gamma\gamma$  production [59], if the photons become collinear, leading to a strong suppression of the LO cross section, as discussed in the following.

Our numerical predictions for the fiducial cross sections are presented in Table 1, where we show the LO, NLO and NNLO results, both combined and split into  $W^+\gamma\gamma$  and  $W^-\gamma\gamma$  production, together with the respective numerical (in brackets) and scale-variation uncertainties.<sup>§</sup> The impact of the NLO corrections is huge, enhancing the LO result by about a factor of 3.6. The NNLO corrections further increase the NLO cross section by about 23%, exceeding the NLO scale-

---

<sup>§</sup> Note that these numbers account for both the  $e^\pm$  and  $\mu^\pm$  decay channels.

$\sigma[\text{fb}]$	$W^+\gamma\gamma$		$W^-\gamma\gamma$		$W\gamma\gamma$	
LO	2.011	+4.8% -5.7%	1.596	+5.5% -6.5%	3.607	+5.1% -6.0%
NLO	6.983	+7.8% -6.3%	5.966	+8.2% -6.6%	12.949	+8.0% -6.5%
NNLO	8.55(2)	+4.5% -4.0%	7.33(2)	+4.4% -4.0%	15.88(3)	+4.5% -4.0%

**Table 1:** Fiducial cross sections for  $W\gamma\gamma$  production in the setup described in the main text. LO, NLO and NNLO predictions for  $W^+\gamma\gamma$ ,  $W^-\gamma\gamma$  and their combination are stated with their seven-point scale variation uncertainties. At NNLO, numerical uncertainties, including the systematic error from the  $r_{\text{cut}} \rightarrow 0$  extrapolation, are shown in brackets. All numbers account for both the  $e^\pm$  and  $\mu^\pm$  decay channels.

variation uncertainties by almost a factor of three. As anticipated, the huge NLO  $K$ -factor can be explained by the opening of the (anti)quark–gluon channel at this perturbative order, and by the LO suppression due to the radiation zero. Indeed, we find that the quark–antiquark channel<sup>¶</sup> accounts for  $\sim 43\%$  of the NLO cross section, while the (anti)quark–gluon channel provides the remaining  $\sim 57\%$ . This pattern is only mildly modified at NNLO, where the quark–antiquark and (anti)quark–gluon channels amount to  $\sim 39\%$  and  $\sim 55\%$  of the NNLO cross section, respectively. Among the new channels at NNLO, the gluon–gluon channel has a negative and quite small ( $\sim -0.7\%$ ) impact, while the off-diagonal (anti)quark-initiated channels contribute the remaining  $\sim 7\%$  of the NNLO cross section.

We briefly comment on the perturbative uncertainties affecting the NNLO predictions reported in Table 1. NNLO is the first perturbative order at which all partonic channels contribute and the corrections to the large (anti)quark–gluon channel, which opens up at NLO, are fully included. Moreover, the radiation zero is already washed out at NLO (see below). Therefore, no further sizeable corrections are expected beyond NNLO. Although scale variations can only provide a lower bound on the true theoretical uncertainty, we can roughly estimate the residual perturbative uncertainty to be at the 5% level. A direct comparison with the measured fiducial cross section reported by ATLAS,  $\sigma = 13.8 \pm 1.1$  (stat) $_{-2.0}^{+2.1}$  (syst)  $\pm 0.1$  (lumi) fb [2], shows good agreement with both our NLO and NNLO predictions, within  $1\sigma$  of the quoted experimental uncertainties.

We now turn to the discussion of differential cross sections. In Figure 2, we show the distributions for the transverse momentum of the leading photon,  $p_{T,\gamma_1}$  (left plot), and the rapidity difference between the charged lepton and the diphoton pair,  $\Delta y_{\ell,\gamma\gamma}$  (right plot). For each distribution, the upper panel displays the absolute predictions, while the lower panel shows the ratios relative to the NLO result. The bands, obtained through the customary seven-point scale variations, are symmetrised. To be precise, we take the maximum among the upward and downward variations and assign it symmetrically to construct our final uncertainty, leaving the central prediction unchanged. The  $p_{T,\gamma_1}$  distribution receives almost flat NNLO corrections of  $\sim 20 - 30\%$  on top of the NLO result. The NNLO (NLO) scale uncertainties range from  $\sim 4\%$  ( $8\%$ ) at low

<sup>¶</sup>By quark–antiquark we refer to the *diagonal* channel that contributes already at the Born level, i.e. with a trivial CKM matrix, the  $u\bar{d}$  and  $d\bar{u}$  channels of the same isospin doublet for  $W^+\gamma\gamma$  and  $W^-\gamma\gamma$ , respectively.

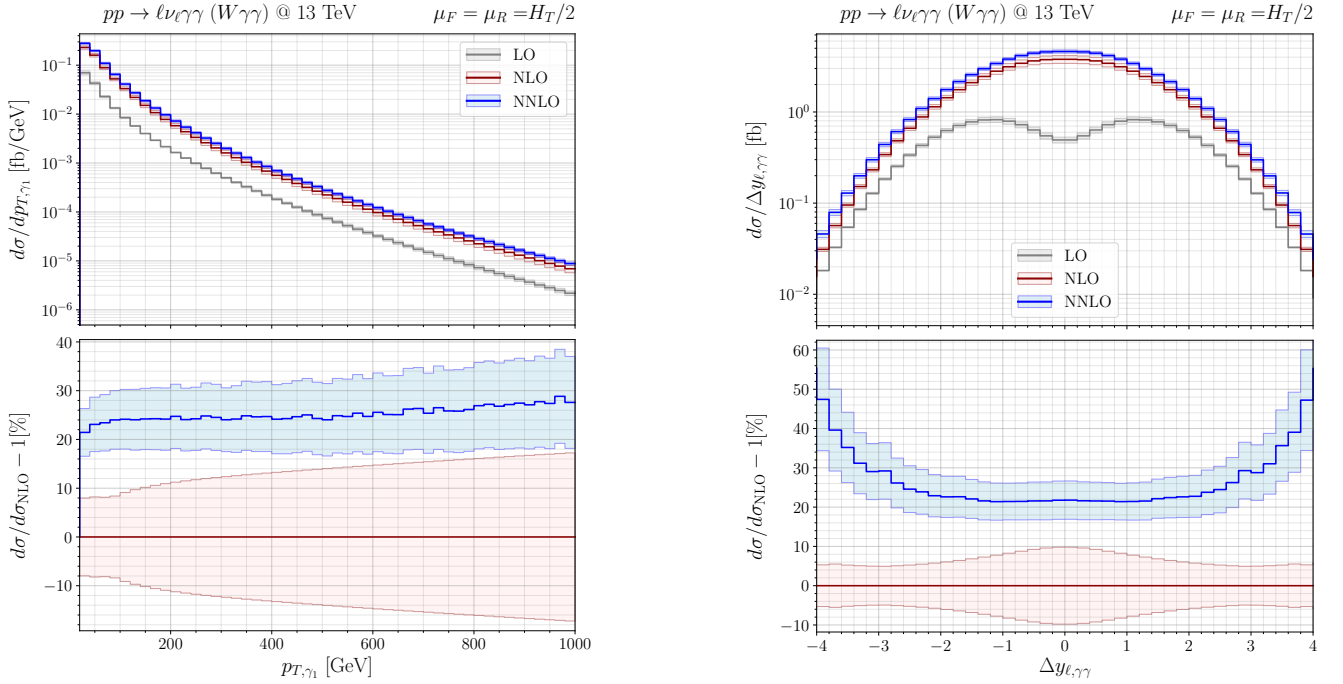


**Figure 2:** Distributions in the transverse momentum of the leading photon,  $p_{T,\gamma_1}$  (left), and in the difference in rapidities between the charged lepton and the diphoton system,  $\Delta y_{\ell,\gamma\gamma}$  (right), are presented for  $W\gamma\gamma$  production. The upper panels show the absolute prediction at LO, NLO and NNLO accuracy, the lower panels relative corrections normalised by the NLO prediction, together with their conventional (symmetrised) seven-point scale-variation bands.

$p_{T,\gamma_1}$  to  $\sim 9\%$  (17%) in the high- $p_{T,\gamma_1}$  region. In the low- $p_{T,\gamma_1}$  region, mostly contributing to the bulk of the cross section, the NLO and NNLO bands do not overlap, consistent with our findings for the fiducial cross sections. On the contrary, the bands become closer in the high- $p_{T,\gamma_1}$  tail and almost overlap at  $p_{T,\gamma_1} \sim 1$  TeV.

The  $\Delta y_{\ell,\gamma\gamma}$  distribution exhibits the well-known radiation-zero pattern [59], responsible for a dip in the LO distribution around  $\Delta y_{\ell,\gamma\gamma} = 0$ . This dip is completely washed out by real-emission contributions beyond LO. Indeed, it is already filled at NLO, with a correction amounting to more than 600% and reflected by the widening of the NLO scale-variation band in the central region. In line with the fiducial NNLO  $K$ -factor, we find that the NLO and NNLO bands do not overlap in the full range.

We finally discuss the impact of the two-loop virtual corrections on the NNLO result. At the fiducial level, they amount to about 1% of the full NNLO prediction. At the differential level, their effect on the  $p_{T,\gamma_1}$  distribution is about 1.5% at the peak, decreasing rapidly to the permille level in the tail. In contrast, for the  $\Delta y_{\ell,\gamma\gamma}$  distribution, their impact amounts to a few permille in the bulk region, but increases up to 7% in the strongly suppressed large- $\Delta y_{\ell,\gamma\gamma}$  region. Overall, assuming that the relative accuracy of the LCA on the two-loop virtual contribution is  $\mathcal{O}(20\%)$ , we can conclude that the ensuing uncertainty on the NNLO predictions is below 1%, much smaller than the residual perturbative uncertainty.

## 4 Summary

In this Letter, we have presented the first NNLO QCD predictions for the production of a  $W$  boson in association with two photons ( $W\gamma\gamma$ ) at the LHC. The calculation has been carried out within the process-independent implementation of the  $q_T$ -subtraction method in the MATRIX framework. Our results are exact, except for the finite part of the two-loop amplitudes, recently computed in the leading-colour approximation, which we have implemented in a dedicated C++ library for efficient numerical evaluation. We find that the well-known radiation zero leads to significant NLO corrections at the fiducial level, while NNLO corrections increase the NLO prediction by about 23% and reduce the perturbative uncertainty to the 5% level. We have studied the impact of QCD radiative corrections for the transverse-momentum distribution of the leading photon and the rapidity separation between the charged lepton and the diphoton system. The latter provides direct sensitivity to the radiation-zero pattern, which is clearly visible at LO, but completely washed out once higher-order corrections are included. Our results provide the first predictions for a triboson process with one off-shell leg at NNLO QCD accuracy. They will enable more stringent tests of the SM, especially in future measurements of quartic gauge couplings as experimental precision improves.

## Acknowledgments

We would like to thank Heather Russell for useful correspondence on Ref. [2], Vasily Sotnikov for advice on and immediate improvements in the `PentagonFunctions++` library. We are further indebted to Simone Zoia for discussions about the two-loop amplitudes exploited in this project. This work is supported in part by the Swiss National Science Foundation (SNF) under contract 200020\_219367. The work of C.S. is partly supported by the Excellence Cluster ORIGINS, funded by the Deutsche Forschungsgemeinschaft (DFG, German Research Foundation) under Germany's Excellence Strategy — EXC-2094-390783311.

## References

- [1] **ATLAS** Collaboration, G. Aad et al., *Evidence of  $W\gamma\gamma$  Production in  $pp$  Collisions at  $s=8$  TeV and Limits on Anomalous Quartic Gauge Couplings with the ATLAS Detector*, *Phys. Rev. Lett.* **115** (2015), no. 3 031802, [[arXiv:1503.03243](#)].
- [2] **ATLAS** Collaboration, G. Aad et al., *Observation of  $W\gamma\gamma$  triboson production in proton-proton collisions at  $\sqrt{s} = 13$  TeV with the ATLAS detector*, *Phys. Lett. B* **848** (2024) 138400, [[arXiv:2308.03041](#)].
- [3] **CMS** Collaboration, A. M. Sirunyan et al., *Measurements of the  $pp \rightarrow W\gamma\gamma$  and  $pp \rightarrow Z\gamma\gamma$  cross sections and limits on anomalous quartic gauge couplings at  $\sqrt{s} = 8$  TeV*, *JHEP* **10** (2017) 072, [[arXiv:1704.00366](#)].
- [4] **CMS** Collaboration, A. Tumasyan et al., *Measurements of the  $pp \rightarrow W^\pm\gamma\gamma$  and  $pp \rightarrow Z\gamma\gamma$  cross sections at  $\sqrt{s} = 13$  TeV and limits on anomalous quartic gauge couplings*, *JHEP* **10** (2021) 174, [[arXiv:2105.12780](#)].
- [5] A. Lazopoulos, K. Melnikov, and F. Petriello, *QCD corrections to tri-boson production*, *Phys. Rev. D* **76** (2007) 014001, [[hep-ph/0703273](#)].
- [6] V. Hankele and D. Zeppenfeld, *QCD corrections to hadronic WWZ production with leptonic decays*, *Phys. Lett. B* **661** (2008) 103–108, [[arXiv:0712.3544](#)].
- [7] T. Binoth, G. Ossola, C. G. Papadopoulos, and R. Pittau, *NLO QCD corrections to tri-boson production*, *JHEP* **06** (2008) 082, [[arXiv:0804.0350](#)].
- [8] F. Campanario, V. Hankele, C. Oleari, S. Prestel, and D. Zeppenfeld, *QCD corrections to charged triple vector boson production with leptonic decay*, *Phys. Rev. D* **78** (2008) 094012, [[arXiv:0809.0790](#)].
- [9] G. Bozzi, F. Campanario, V. Hankele, and D. Zeppenfeld, *NLO QCD corrections to  $W^+W^-\gamma$  and  $ZZ\gamma$  production with leptonic decays*, *Phys. Rev. D* **81** (2010) 094030, [[arXiv:0911.0438](#)].
- [10] G. Bozzi, F. Campanario, M. Rauch, H. Rzehak, and D. Zeppenfeld, *NLO QCD corrections to  $W^\pm Z\gamma$  production with leptonic decays*, *Phys. Lett. B* **696** (2011) 380–385, [[arXiv:1011.2206](#)].
- [11] G. Bozzi, F. Campanario, M. Rauch, and D. Zeppenfeld,  *$W^{+-}\gamma\gamma$  production with leptonic decays at NLO QCD*, *Phys. Rev. D* **83** (2011) 114035, [[arXiv:1103.4613](#)].
- [12] U. Baur, D. Wackerroth, and M. M. Weber, *Radiative corrections to  $W$  gamma gamma production at the LHC*, *PoS RADCOR2009* (2010) 067, [[arXiv:1001.2688](#)].
- [13] G. Bozzi, F. Campanario, M. Rauch, and D. Zeppenfeld,  *$Z\gamma\gamma$  production with leptonic decays and triple photon production at next-to-leading order QCD*, *Phys. Rev. D* **84** (2011) 074028, [[arXiv:1107.3149](#)].

- [14] J. M. Campbell, H. B. Hartanto, and C. Williams, *Next-to-leading order predictions for  $Z\gamma$ +jet and  $Z\gamma\gamma$  final states at the LHC*, *JHEP* **11** (2012) 162, [[arXiv:1208.0566](#)].
- [15] E. Celada, G. Durieux, K. Mimasu, and E. Vryonidou, *Triboson production in the SMEFT*, *JHEP* **12** (2024) 055, [[arXiv:2407.09600](#)].
- [16] M. Schönherr, *Next-to-leading order electroweak corrections to off-shell WWW production at the LHC*, *JHEP* **07** (2018) 076, [[arXiv:1806.00307](#)].
- [17] S. Dittmaier, G. Knippen, and C. Schwan, *Next-to-leading-order QCD and electroweak corrections to triple-W production with leptonic decays at the LHC*, *JHEP* **02** (2020) 003, [[arXiv:1912.04117](#)].
- [18] H. Cheng and D. Wackerroth, *NLO electroweak and QCD corrections to the production of a photon with three charged lepton plus missing energy at the LHC*, *Phys. Rev. D* **105** (2022), no. 9 096009, [[arXiv:2112.12052](#)].
- [19] A. Denner, M. Pellen, M. Schönherr, and S. Schumann, *Tri-boson and WH production in the  $W^+W^+jj$  channel: predictions at full NLO accuracy and beyond*, *JHEP* **08** (2024) 043, [[arXiv:2406.11516](#)].
- [20] A. Denner, D. Lombardi, S. L. P. Chavez, and G. Pelliccioli, *NLO corrections to triple vector-boson production in final states with three charged leptons and two jets*, *JHEP* **09** (2024) 187, [[arXiv:2407.21558](#)].
- [21] N. Greiner and M. Schönherr, *NLO QCD+EW corrections to diphoton production in association with a vector boson*, *JHEP* **01** (2018) 079, [[arXiv:1710.11514](#)].
- [22] S. Catani, L. Cieri, D. de Florian, G. Ferrera, and M. Grazzini, *Diphoton production at hadron colliders: a fully-differential QCD calculation at NNLO*, *Phys. Rev. Lett.* **108** (2012) 072001, [[arXiv:1110.2375](#)].
- [23] M. Grazzini, S. Kallweit, D. Rathlev, and A. Torre,  *$Z\gamma$  production at hadron colliders in NNLO QCD*, *Phys. Lett.* **B731** (2014) 204–207, [[arXiv:1309.7000](#)].
- [24] M. Grazzini, S. Kallweit, and D. Rathlev,  *$W\gamma$  and  $Z\gamma$  production at the LHC in NNLO QCD*, *JHEP* **07** (2015) 085, [[arXiv:1504.01330](#)].
- [25] J. M. Campbell, R. K. Ellis, Y. Li, and C. Williams, *Predictions for diphoton production at the LHC through NNLO in QCD*, *JHEP* **07** (2016) 148, [[arXiv:1603.02663](#)].
- [26] M. Grazzini, S. Kallweit, and M. Wiesemann, *Fully differential NNLO computations with MATRIX*, *Eur. Phys. J. C* **78** (2018), no. 7 537, [[arXiv:1711.06631](#)].
- [27] S. Catani, L. Cieri, D. de Florian, G. Ferrera, and M. Grazzini, *Diphoton production at the LHC: a QCD study up to NNLO*, *JHEP* **04** (2018) 142, [[arXiv:1802.02095](#)].
- [28] J. M. Campbell, T. Neumann, and C. Williams,  *$Z\gamma$  Production at NNLO Including Anomalous Couplings*, *JHEP* **11** (2017) 150, [[arXiv:1708.02925](#)].

- [29] J. M. Campbell, G. De Laurentis, R. K. Ellis, and S. Seth, *The  $pp \rightarrow W(\rightarrow l\nu) + \gamma$  process at next-to-next-to-leading order*, *JHEP* **07** (2021) 079, [[arXiv:2105.00954](#)].
- [30] H. A. Chawdhry, M. L. Czakon, A. Mitov, and R. Poncelet, *NNLO QCD corrections to three-photon production at the LHC*, *JHEP* **02** (2020) 057, [[arXiv:1911.00479](#)].
- [31] S. Kallweit, V. Sotnikov, and M. Wiesemann, *Triphoton production at hadron colliders in NNLO QCD*, *Phys. Lett. B* **812** (2021) 136013, [[arXiv:2010.04681](#)].
- [32] S. Abreu, G. De Laurentis, H. Ita, M. Klinkert, B. Page, and V. Sotnikov, *Two-Loop QCD Corrections for Three-Photon Production at Hadron Colliders*, [arXiv:2305.17056](#).
- [33] **ATLAS** Collaboration, M. Aaboud et al., *Measurement of the production cross section of three isolated photons in  $pp$  collisions at  $\sqrt{s} = 8$  TeV using the ATLAS detector*, *Phys. Lett. B* **781** (2018) 55–76, [[arXiv:1712.07291](#)].
- [34] S. Badger, H. B. Hartanto, Z. Wu, Y. Zhang, and S. Zoia, *Two-loop amplitudes for  $\mathcal{O}(\alpha_s^2)$  corrections to  $W\gamma\gamma$  production at the LHC*, [arXiv:2409.08146](#).
- [35] S. Catani and M. Grazzini, *An NNLO subtraction formalism in hadron collisions and its application to Higgs boson production at the LHC*, *Phys. Rev. Lett.* **98** (2007) 222002, [[hep-ph/0703012](#)].
- [36] S. Catani and M. H. Seymour, *The Dipole formalism for the calculation of QCD jet cross-sections at next-to-leading order*, *Phys. Lett. B* **378** (1996) 287–301, [[hep-ph/9602277](#)].
- [37] S. Catani and M. H. Seymour, *A General algorithm for calculating jet cross-sections in NLO QCD*, *Nucl. Phys. B* **485** (1997) 291–419, [[hep-ph/9605323](#)]. [Erratum: *Nucl.Phys.B* 510, 503–504 (1998)].
- [38] M. A. Ebert and F. J. Tackmann, *Impact of isolation and fiducial cuts on  $q_T$  and  $N$ -jettiness subtractions*, *JHEP* **03** (2020) 158, [[arXiv:1911.08486](#)].
- [39] F. Cascioli, P. Maierhöfer, and S. Pozzorini, *Scattering Amplitudes with Open Loops*, *Phys. Rev. Lett.* **108** (2012) 111601, [[arXiv:1111.5206](#)].
- [40] F. Buccioni, S. Pozzorini, and M. Zoller, *On-the-fly reduction of open loops*, *Eur. Phys. J. C* **78** (2018), no. 1 70, [[arXiv:1710.11452](#)].
- [41] F. Buccioni, J.-N. Lang, J. M. Lindert, P. Maierhöfer, S. Pozzorini, H. Zhang, and M. F. Zoller, *OpenLoops 2*, *Eur. Phys. J. C* **79** (2019), no. 10 866, [[arXiv:1907.13071](#)].
- [42] S. Actis, A. Denner, L. Hofer, J.-N. Lang, A. Scharf, and S. Uccirati, *RECOLA: REcursive Computation of One-Loop Amplitudes*, *Comput. Phys. Commun.* **214** (2017) 140–173, [[arXiv:1605.01090](#)].
- [43] A. Denner, J.-N. Lang, and S. Uccirati, *Recola2: REcursive Computation of One-Loop Amplitudes 2*, *Comput. Phys. Commun.* **224** (2018) 346–361, [[arXiv:1711.07388](#)].

- [44] A. Denner, S. Dittmaier, and L. Hofer, *Collier: a fortran-based Complex One-Loop Library in Extended Regularizations*, *Comput. Phys. Commun.* **212** (2017) 220–238, [[arXiv:1604.06792](#)].
- [45] L. Buonocore, S. Devoto, S. Kallweit, J. Mazzitelli, L. Rottoli, and C. Savoini, *Associated production of a W boson and massive bottom quarks at next-to-next-to-leading order in QCD*, *Phys. Rev. D* **107** (2023), no. 7 074032, [[arXiv:2212.04954](#)].
- [46] L. Buonocore, S. Devoto, M. Grazzini, S. Kallweit, J. Mazzitelli, L. Rottoli, and C. Savoini, *Precise Predictions for the Associated Production of a W Boson with a Top-Antitop Quark Pair at the LHC*, *Phys. Rev. Lett.* **131** (2023), no. 23 231901, [[arXiv:2306.16311](#)].
- [47] S. Devoto, M. Grazzini, S. Kallweit, J. Mazzitelli, and C. Savoini, *Precise predictions for  $t\bar{t}H$  production at the LHC: inclusive cross section and differential distributions*, *JHEP* **03** (2025) 189, [[arXiv:2411.15340](#)].
- [48] T. Becher and M. Neubert, *Infrared singularities of scattering amplitudes in perturbative QCD*, *Phys. Rev. Lett.* **102** (2009) 162001, [[arXiv:0901.0722](#)]. [Erratum: *Phys.Rev.Lett.* 111, 199905 (2013)].
- [49] The PENTAGONFUNCTIONS++ library, by V. Sotnikov, is publicly available at <https://gitlab.com/pentagon-functions/PentagonFunctions-cpp>.
- [50] D. Chicherin and V. Sotnikov, *Pentagon Functions for Scattering of Five Massless Particles*, *JHEP* **20** (2020) 167, [[arXiv:2009.07803](#)].
- [51] D. Chicherin, V. Sotnikov, and S. Zoia, *Pentagon functions for one-mass planar scattering amplitudes*, *JHEP* **01** (2022) 096, [[arXiv:2110.10111](#)].
- [52] S. Abreu, D. Chicherin, H. Ita, B. Page, V. Sotnikov, W. Tschernow, and S. Zoia, *All Two-Loop Feynman Integrals for Five-Point One-Mass Scattering*, *Phys. Rev. Lett.* **132** (2024), no. 14 141601, [[arXiv:2306.15431](#)].
- [53] S. Frixione, *Isolated photons in perturbative QCD*, *Phys. Lett. B* **429** (1998) 369–374, [[hep-ph/9801442](#)].
- [54] **Particle Data Group** Collaboration, C. Patrignani et al., *Review of Particle Physics*, *Chin. Phys.* **C40** (2016), no. 10 100001.
- [55] A. Denner, S. Dittmaier, M. Roth, and L. H. Wieders, *Electroweak corrections to charged-current  $e^+e^- \rightarrow 4$  fermion processes: Technical details and further results*, *Nucl. Phys.* **B724** (2005) 247–294, [[hep-ph/0505042](#)]. [Erratum: *Nucl. Phys.* B854, 504 (2012)].
- [56] **NNPDF** Collaboration, R. D. Ball et al., *The path to proton structure at 1% accuracy*, *Eur. Phys. J. C* **82** (2022), no. 5 428, [[arXiv:2109.02653](#)].
- [57] A. Buckley, J. Ferrando, S. Lloyd, K. Nordström, B. Page, M. Rüfenacht, M. Schönherr, and G. Watt, *LHAPDF6: parton density access in the LHC precision era*, *Eur. Phys. J. C* **75** (2015) 132, [[arXiv:1412.7420](#)].

- [58] K. O. Mikaelian, M. A. Samuel, and D. Sahdev, *The Magnetic Moment of Weak Bosons Produced in  $p p$  and  $p$  anti- $p$  Collisions*, *Phys. Rev. Lett.* **43** (1979) 746.
- [59] U. Baur, T. Han, N. Kauer, R. Sobey, and D. Zeppenfeld,  *$W\gamma\gamma$  production at the Fermilab Tevatron collider: Gauge invariance and radiation amplitude zero*, *Phys. Rev. D* **56** (1997) 140–150, [[hep-ph/9702364](#)].